THE EUROPEAN
PHYSICAL JOURNAL C

CrossMark

Regular Article - Theoretical Physics

Status of the $B \to K^* \mu^+ \mu^-$ anomaly after Moriond 2017

Wolfgang Altmannshofer[1,a], **Christoph Niehoff**[2,b], **Peter Stangl**[2,c], **David M. Straub**[2,d]

[1] Department of Physics, University of Cincinnati, Cincinnati, OH 45221, USA
[2] Excellence Cluster Universe, Boltzmannstr. 2, 85748 Garching, Germany

Abstract Motivated by recent results by the ATLAS and CMS collaborations on the angular distribution of the $B \to K^* \mu^+ \mu^-$ decay, we perform a state-of-the-art analysis of rare B meson decays based on the $b \to s\mu\mu$ transition. Using standard estimates of hadronic uncertainties, we confirm the presence of a sizeable discrepancy between data and SM predictions. We do not find evidence for a q^2 or helicity dependence of the discrepancy. The data can be consistently described by new physics in the form of a four-fermion contact interaction $(\bar{s}\gamma_\alpha P_L b)(\bar{\mu}\gamma^\alpha \mu)$. Assuming that the new physics affects decays with muons but not with electrons, we make predictions for a variety of theoretically clean observables sensitive to violation of lepton flavour universality.

1 Introduction

The angular distribution of the decay $B \to K^* \mu^+ \mu^-$ was known to be a key probe of physics beyond the Standard Model (SM) at the LHC already before its start (see e.g. [1–5]) and the observable S_5 was recognized early on to be particularly promising [5,6]. A different normalization for this observable, reducing form factor uncertainties, was suggested in Ref. [7], rebranded as P_5'. While B factory and Tevatron measurements of the forward-backward asymmetry and longitudinal polarization fraction had been in agreement with SM expectations [8–10], in 2013, the LHCb collaboration announced the observation of a tension in the observable P_5' at the level of around three standard deviations. It was quickly recognized [11] that a new physics (NP) contribution to the Wilson coefficient C_9 of a semi-leptonic vector operator was able to explain this "$B \to K^* \mu^+ \mu^-$ anomaly", confirmed few days later by an independent analysis [12] and

also by other groups with different methods [13,14]. Further measurements have shown additional tensions, e.g. branching ratio measurements in $B \to K \mu^+ \mu^-$ and $B_s \to \phi \mu^+ \mu^-$ [15,16], as well as, most notably, a hint for lepton flavour non-universality in $B^+ \to K^+ \ell^+ \ell^-$ decays [17]. While progress has also been made on the theory side, most notably improved $B \to K^*$ form factors from lattice QCD (LQCD) [18,19] and light-cone sum rules (LCSR) [20], the "anomaly" has also led to a renewed scrutiny of theoretical uncertainties due to form factors [21–23] as well as non-factorizable hadronic effects [24–26] (cf. also the earlier work in [27–30]).

In 2015, the LHCb collaboration presented their $B \to K^* \mu^+ \mu^-$ angular analysis based on the full Run 1 data set, confirming the tension found earlier [31]. Several updated global analyses have confirmed that a consistent description of the tensions in terms of NP is possible [32–34], while an explanation in terms of an unexpectedly large hadronic effect cannot be excluded. Recent analyses by Belle [35,36] also seem to indicate tensions in angular observables consistent with LHCb. At Moriond Electroweak 2017, ATLAS [37] and CMS [38] finally presented their preliminary results for the angular observables based on the full Run 1 data sets. The aim of the present paper is to reconsider the status of the $B \to K^* \mu^+ \mu^-$ anomaly in view of these results. Our analysis is built on our previous global analyses of NP in $b \to s$ transitions [12,32,39,40] and makes use of the open source code flavio [41].

2 Effective Hamiltonian and observables

The effective Hamiltonian for $b \to s$ transitions can be written as

$$\mathcal{H}_{\text{eff}} = -\frac{4\,G_F}{\sqrt{2}} V_{tb} V_{ts}^* \frac{e^2}{16\pi^2} \sum_i (C_i O_i + C_i' O_i') + \text{h.c.} \quad (1)$$

and we consider NP effects in the following set of dimension-6 operators:

[a] e-mail: altmanwg@ucmail.uc.edu

[b] e-mail: christoph.niehoff@tum.de

[c] e-mail: peter.stangl@tum.de

[d] e-mail: david.straub@tum.de

$$O_9 = (\bar{s}\gamma_\mu P_L b)(\bar{\ell}\gamma^\mu \ell), \qquad O'_9 = (\bar{s}\gamma_\mu P_R b)(\bar{\ell}\gamma^\mu \ell),$$
(2)

$$O_{10} = (\bar{s}\gamma_\mu P_L b)(\bar{\ell}\gamma^\mu \gamma_5 \ell), \quad O'_{10} = (\bar{s}\gamma_\mu P_R b)(\bar{\ell}\gamma^\mu \gamma_5 \ell).$$
(3)

We neither consider new physics in scalar operators, as they are strongly constrained by $B_s \to \mu^+\mu^-$ (see [42] for a recent analysis), nor in dipole operators, which are strongly constrained by inclusive and exclusive radiative decays (see [43] for a recent analysis). We also do not consider new physics in four-quark operators, although an effect in certain $b \to c\bar{c}s$ operators could potentially relax some of the tensions in $B \to K^*\mu^+\mu^-$ angular observables [44].

In our numerical analysis, we include the following observables.

- Angular observables in $B^0 \to K^{*0}\mu^+\mu^-$ measured by CDF [45], LHCb [31], ATLAS* [37], and CMS* [38,46, 47],
- $B^{0,\pm} \to K^{*0,\pm}\mu^+\mu^-$ branching ratios by LHCb* [15, 48], CMS [46,47], and CDF [45],
- $B^{0,\pm} \to K^{0,\pm}\mu^+\mu^-$ branching ratios by LHCb [15] and CDF [45],
- $B_s \to \phi\mu^+\mu^-$ branching ratio by LHCb* [16] and CDF [45],
- $B_s \to \phi\mu^+\mu^-$ angular observables by LHCb* [16],
- the branching ratio of the inclusive decay $B \to X_s\mu^+\mu^-$ measured by BaBar [49].

Items marked with an asterisk have been updated since our previous global fit [32]. Concerning $B^0 \to K^{*0}\mu^+\mu^-$, both LHCb and ATLAS have performed measurements of CP-averaged angular observables S_i as well as of the closely related "optimized" observables P'_i. While LHCb gives also the full correlation matrices and the choice of basis is thus irrelevant (up to non-Gaussian effects which are anyway impossible to take into account using publicly available information), ATLAS does not give correlations, so the choice can make a difference in principle. We have chosen to use the P'_i measurements, but we have explicitly checked that the best-fit regions and pulls do not change significantly when using the S_i observables.

We do *not* include the following measurements.

- Angular observables in $B \to K\mu^+\mu^-$, which are only relevant in the presence of scalar or tensor operators [50],
- measurements of lepton-averaged observables, as we want to focus on new physics in $b \to s\mu^+\mu^-$ transitions,
- the Belle measurement of $B \to K^*\mu^+\mu^-$ angular observables [36], as it contains an unknown mixture of

B^0 and $B^\pm$ decays that receive different non-factorizable corrections at low q^2,
- the LHCb measurement of the decay $\Lambda_b \to \Lambda\mu^+\mu^-$ [51], as it still suffers from large experimental uncertainties and the central values of the measurement are not compatible with any viable short-distance hypothesis [52].

We do not make use of the LHCb analysis attempting to separately extract the short- and long-distance contributions to the $B^+ \to K^+\mu^+\mu^-$ decay [53], but we note that these results are in qualitative agreement with our estimates of long-distance contributions to this decay. Finally, we do not include the decay $B_s \to \mu^+\mu^-$ in our fit, as it can be affected by scalar operators, as discussed above.

For all these semi-leptonic observables, which are measured in bins of q^2, we discard the following bins from our numerical analysis.

- Bins below the J/ψ resonance that extend above 6 GeV^2. In this region, theoretical calculations based on QCD factorization are not reliable [54].
- Bins above the $\psi(2S)$ resonance that are less than 4 GeV^2 wide. This is because theoretical predictions are only valid for sufficiently global, i.e. q^2-integrated, observables in this region [28].
- Bins with upper boundary *at or below* 1 GeV^2, because this region is dominated by the photon pole and thus by dipole operators, while we are interested in the effect of semi-leptonic operators in this work.

For the SM predictions of these observables, we refer the reader to Refs. [20,32], where the calculations, inputs, and parametrization of hadronic uncertainties have been discussed in detail. Our predictions are based on the implementation of these calculations in the open source code `flavio` [41]. With respect to our previous analysis [32], we use improved predictions for $B \to K^*$ and $B_s \to \phi$ form factors from [20] and $B \to K$ form factors from [55]. Note that the $B \to K$ form factors from [55] have substantially smaller uncertainties compared to the ones used in [32], which were based on the results in [56–58]. The increased tension due to these form factors was also pointed out in [59].

3 Results and discussion

From the measurements and theory predictions, we construct a χ^2 function where theory uncertainties are combined with experimental uncertainties, such that the χ^2 only depends on the Wilson coefficients. Both for the theoretical and the experimental uncertainties, we take into account all known correlations and approximate the uncertainties as (multivariate) Gaussians, and we neglect the dependence of the uncer-

Table 1 Best-fit values and pulls in sigma between the best-fit point and the SM point for scenarios with NP in one or two Wilson coefficients. For the one-dimensional cases, we also show the 1 and 2σ best-fit ranges. For two of the two-dimensional cases, the best-fit regions are shown in Fig. 1.

Coeff.	Best fit	1σ	2σ	Pull
C_9^{NP}	-1.21	$[-1.41, -1.00]$	$[-1.61, -0.77]$	5.2σ
C_9'	$+0.19$	$[-0.01, +0.40]$	$[-0.22, +0.60]$	0.9σ
C_{10}^{NP}	$+0.79$	$[+0.55, +1.05]$	$[+0.32, +1.31]$	3.4σ
C_{10}'	-0.10	$[-0.26, +0.07]$	$[-0.42, +0.24]$	0.6σ
$C_9^{\mathrm{NP}} = C_{10}^{\mathrm{NP}}$	-0.30	$[-0.50, -0.08]$	$[-0.69, +0.18]$	1.3σ
$C_9^{\mathrm{NP}} = -C_{10}^{\mathrm{NP}}$	-0.67	$[-0.83, -0.52]$	$[-0.99, -0.38]$	4.8σ
$C_9' = C_{10}'$	$+0.06$	$[-0.18, +0.30]$	$[-0.42, +0.55]$	0.3σ
$C_9' = -C_{10}'$	$+0.08$	$[-0.02, +0.18]$	$[-0.12, +0.28]$	0.8σ
$C_9^{\mathrm{NP}}, C_{10}^{\mathrm{NP}}$	$(-1.15, +0.26)$	–	–	5.0σ
C_9^{NP}, C_9'	$(-1.25, +0.59)$	–	–	5.3σ
$C_9^{\mathrm{NP}}, C_{10}'$	$(-1.34, -0.39)$	–	–	5.4σ
$C_9', C_{10}^{\mathrm{NP}}$	$(+0.25, +0.83)$	–	–	3.2σ
C_9', C_{10}'	$(+0.23, +0.04)$	–	–	0.5σ
$C_{10}^{\mathrm{NP}}, C_{10}'$	$(+0.79, -0.05)$	–	–	3.0σ

tainties on the NP contributions. This procedure, which was proposed in [32] and later adopted by other groups [33] is implemented in `flavio` as the `FastFit` class.

From the observable selection discussed in Sect. 2, we end up with a total number of 86 measurements of 81 distinct observables. These observables are not independent, but their theoretical and experimental uncertainties are correlated. We take into account the experimental correlations where known (this is the case only for the angular analyses of $B \to K^*\mu^+\mu^-$ and $B_s \to \phi\mu^+\mu^-$ by LHCb), and include all theory correlations. Before considering NP effects, we can evaluate the χ^2 function within the SM to get a feeling of the agreement of the data with the SM hypothesis. However, this absolute χ^2 is not uniquely defined. For instance, averaging multiple measurements of identical observables by different experiments before they enter the χ^2, we obtain $\chi^2_{\mathrm{SM}} = 98.5$ for 81 observables. Adding all individual measurements separately instead, we obtain $\chi^2_{\mathrm{SM}} = 100.6$ for 86 measurements. For the $\Delta\chi^2$ used in the remainder of the analysis, these procedures are equivalent.

3.1 New physics in individual Wilson coefficients

As a first step, we switch on NP contributions in individual Wilson coefficients, determine the best-fit point in the one- or two-dimensional space, and evaluate the χ^2 difference $\Delta\chi^2$ with respect to the SM point. The "pull" in σ is then defined as $\sqrt{\Delta\chi^2}$ in the one-dimensional case, while in the two-dimensional case it can be evaluated using the inverse cumulative distribution function of the χ^2 distribution with two degrees of freedom; for instance, $\Delta\chi^2 \approx 2.3$ for 1σ.

The results are shown in Table 1. We make the following observations.

- The strongest pull is obtained in the scenario with NP in C_9 only and it amounts to slightly more than five standard deviations. Consistently with fits before the updated ATLAS and CMS measurements, the best-fit point corresponds to a value around $C_9 \sim -1$, i.e. destructive interference with the SM Wilson coefficient. The increase in the significance for a non-standard C_9 (3.9σ in [32] vs. 5.2σ here) can be largely traced back to the new and more precise form factors we are using, with only a moderate impact of the added experimental measurements.
- A scenario with NP in C_{10} only also gives an improved fit, although less significantly than the C_9 scenario. We note that this suppression of C_{10} by roughly 20% would imply a suppression of the $B_s \to \mu^+\mu^-$ branching ratio—which, we stress again, we have not included in the fit—by roughly 35%.
- A scenario with $C_9^{\mathrm{NP}} = -C_{10}^{\mathrm{NP}}$, which is well motivated by models with mediators coupling only to left-handed leptons, leads to a comparably good fit as the C_9-only scenario.

To understand where the large global tension comes from, it is instructive to perform one-dimensional fits with NP in C_9 using only a subset of the data. We find for instance that

- measurements of the $B_s \to \phi\mu^+\mu^-$ branching ratio alone lead to a pull of 3.5σ,
- all branching ratio measurements combined lead to a pull of 4.6σ,
- the $B \to K^*\mu^+\mu^-$ angular analysis by LHCb alone leads to a pull of 3.0σ,
- the new $B \to K^*\mu^+\mu^-$ angular analysis by CMS reduces the pull, but the new ATLAS measurement increases it.
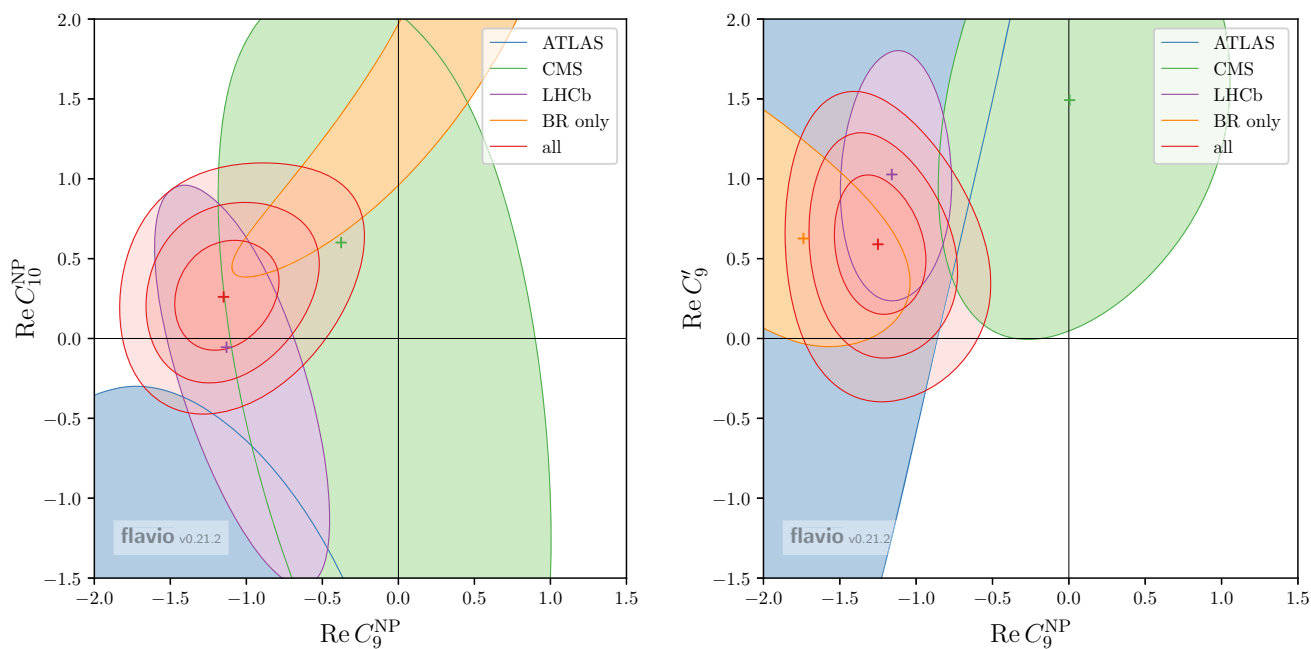
Fig. 1 Two-dimensional constraints in the plane of NP contributions to the real parts of the Wilson coefficients C_9 and C_{10} (*left*) or C_9 and C_9' (*right*), assuming all other Wilson coefficients to be SM-like. For the constraints from the $B \to K^* \mu^+ \mu^-$ and $B_s \to \phi \mu^+ \mu^-$ angular observables from individual experiments as well as for the constraints from branching ratio measurements of all experiments ("BR only"), we show the 1σ ($\Delta\chi^2 \approx 2.3$) contours, while for the global fit ("all"), we show the 1, 2, and 3σ contours

The significance of the tension between the branching ratio measurements and the corresponding SM predictions depends strongly on the form factors used. To estimate the possible impact of underestimated form factor uncertainties, we repeat the fit with NP in C_9, doubling the form factor uncertainties with respect to our nominal fit. We find that the pull is reduced from 5.2σ to 4.0σ. Significant tensions remain in this scenario, indicating that underestimated form factor uncertainties are likely not the only source of the discrepancies.

We also perform a fit doubling the uncertainties of the non-factorizable hadronic corrections (see [32] for details of how we estimate these uncertainties). We find a reduced pull of 4.4σ.

3.2 New physics in pairs of Wilson coefficients

Next, we consider pairs of Wilson coefficients. In the last four rows of Table 1, we show the best-fit points and pulls for four different scenarios. We observe that adding one of the primed coefficients does not improve the fit substantially.

In Fig. 1 we plot contours of constant $\Delta\chi^2$ in the planes of two Wilson coefficients for the scenarios with NP in C_9 and C_{10} or in C_9 and C_9', assuming the remaining coefficients to be SM-like. In both plots, we show the 1, 2, and 3σ contours for the global fit, but also 1σ contours showing the constraints coming from the angular analyses of individual experiments, as well as from branching ratio measurements of all experiments.

We observe that the individual constraints are all compatible with the global fit at the 1σ or 2σ level. While the CMS angular analysis shows good agreement with the SM expectations, all other individual constraints show a deviation from the SM. In view of their precision, the angular analysis and branching ratio measurements of LHCb still dominate the global fit (cf. Figs. 5, 7, 6 and 8), leading to an allowed region similar to previous analyses. We do not find any significant preference for non-zero NP contributions in C_{10} or C_9' in these two simple scenarios.

Similarly to our analysis of scenarios with NP in one Wilson coefficient, we repeat the fits doubling the form factor uncertainties and doubling the uncertainties of non-factorizable corrections. For NP in C_9 and C_{10}, we find that the pull is reduced from 5.0σ to 3.7σ and 4.1σ, respectively. For NP in C_9 and C_9' the pull is reduced from 5.3σ to 4.1σ and 4.4σ, respectively. The impact of the inflated uncertainties is also illustrated in Fig. 2. Doubling the hadronic uncertainties is not sufficient to achieve agreement between data and SM predictions at the 3σ level.

3.3 New physics or hadronic effects?

It is conceivable that hadronic effects that are largely underestimated could mimic new physics in the Wilson coeffi-
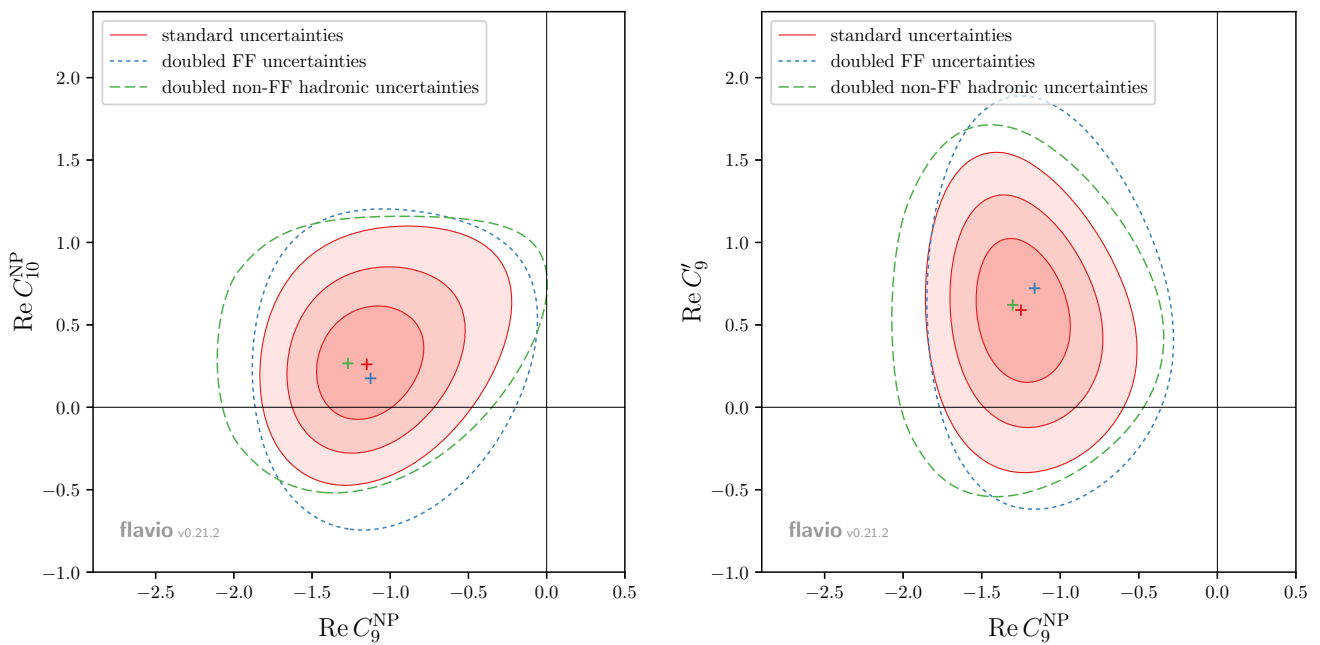
Fig. 2 Allowed regions in the Re($C_9^{\rm NP}$)-Re($C_{10}^{\rm NP}$) plane (*left*) and the Re($C_9^{\rm NP}$)-Re(C_9') plane (*right*). In *red* the 1σ, 2σ, and 3σ best-fit regions with nominal hadronic uncertainties. The *green dashed* and *blue short-dashed* contours correspond to the 3σ regions in scenarios with doubled uncertainties from non-factorizable corrections and doubled form factor uncertainties, respectively.
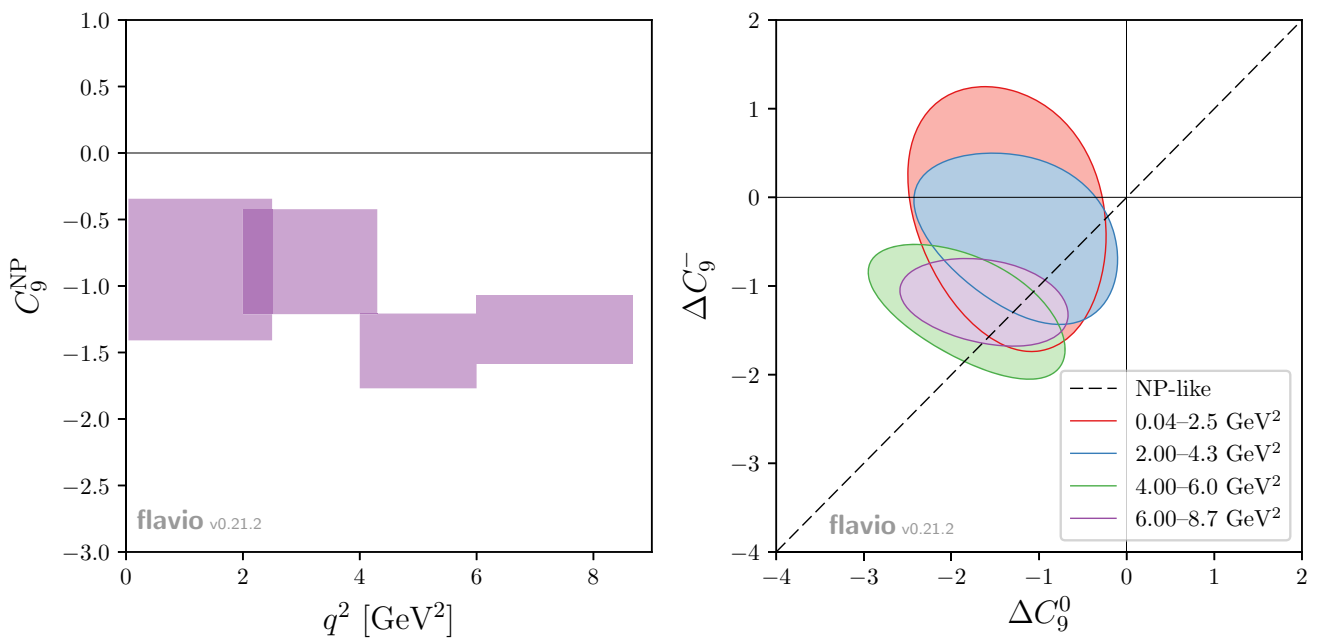

Fig. 3 *Left* preferred 1σ ranges for a new physics contribution to C_9 from fits in different q^2 bins. *Right* preferred 1σ ranges for helicity dependent contributions to C_9 from fits in different q^2 bins. The *dashed diagonal line* corresponds to a helicity universal contribution, as predicted by new physics

cient C_9 [24]. As first quantified in [60] and later considered in [23,25,26,33], there are ways to test this possibility by studying the q^2 and helicity dependence of a non-standard effect in C_9.

Without loss of generality, any photon-mediated hadronic contribution to the $B \to K^* \mu^+ \mu^-$ helicity amplitudes can be expressed as a q^2 and helicity dependent shift in C_9, since the photon has a vector-like coupling to leptons and flavour-violation always involves left-handed quarks in the SM. A

Table 2 Predictions for lepton flavour universality ratios and differences in new physics models with muon specific contributions to C_9 and C_{10}, or C_9 and C_9'. The superscripts on the observables indicate the q^2 range in GeV^2

| | (i) $C_9^\mu - C_{10}^\mu$ fit | | (ii) $C_9^\mu - C_9'^\mu$ fit | |
	1σ	2σ	1σ	2σ
$R_K^{[1,6]}$	$0.70^{+0.09}_{-0.05}$	$[0.59, 0.86]$	$0.76^{+0.04}_{-0.02}$	$[0.71, 0.84]$
$R_K^{[15,22]}$	$0.70^{+0.09}_{-0.05}$	$[0.59, 0.87]$	$0.69^{+0.05}_{-0.03}$	$[0.64, 0.79]$
$R_{K^*}^{[0.045,1.1]}$	$0.87^{+0.02}_{-0.02}$	$[0.83, 0.92]$	$0.86^{+0.02}_{-0.01}$	$[0.85, 0.89]$
$R_{K^*}^{[1,6]}$	$0.77^{+0.08}_{-0.06}$	$[0.64, 0.92]$	$0.76^{+0.04}_{-0.04}$	$[0.72, 0.84]$
$R_{K^*}^{[15,19]}$	$0.70^{+0.09}_{-0.05}$	$[0.59, 0.86]$	$0.71^{+0.03}_{-0.04}$	$[0.64, 0.79]$
$R_\phi^{[1,6]}$	$0.76^{+0.08}_{-0.06}$	$[0.63, 0.91]$	$0.75^{+0.04}_{-0.03}$	$[0.70, 0.83]$
$R_\phi^{[15,19]}$	$0.70^{+0.09}_{-0.05}$	$[0.59, 0.86]$	$0.71^{+0.04}_{-0.05}$	$[0.63, 0.79]$
$D_{P_5'}^{[1,6]}$	$0.29^{+0.11}_{-0.05}$	$[0.15, 0.47]$	$0.35^{+0.07}_{-0.07}$	$[0.22, 0.49]$
$D_{S_5}^{[1,6]}$	$0.12^{+0.05}_{-0.02}$	$[0.06, 0.2]$	$0.15^{+0.03}_{-0.03}$	$[0.09, 0.21]$
$D_{A_{\mathrm{FB}}}^{[1,6]}$	$-0.09^{+0.02}_{-0.02}$	$[-0.13, -0.04]$	$-0.10^{+0.02}_{-0.02}$	$[-0.14, -0.06]$

new physics contribution to the Wilson coefficient C_9 is by definition independent of the di-muon invariant mass q^2, and it is universal for all three helicity amplitudes. For hadronic effects, the situation is rather different. It can be argued that hadronic effects in the $\lambda = +$ helicity amplitudes are suppressed [30] and a priori there is no reason to expect that hadronic effects in the $\lambda = 0$ and $\lambda = -$ amplitudes are of the same size. Moreover, one would naively expect that hadronic effects that can arise e.g. from charm loops show a non-trivial q^2 behaviour. However, we would like to stress that no robust predictions about the precise properties of the hadronic effects can be made at present.

Another interesting possibility is to have NP contributions in $b \to c\bar{c}s$ operators as speculated in [24] and recently worked out in [44]. In this case, the shift in C_9 would be q^2 dependent, but helicity *independent* up to corrections of order α_s and $\Lambda_{\mathrm{QCD}}/m_b$.

In order to understand if the data shows preference for a non-trivial q^2 dependence, we perform a series of fits to non-standard contributions to the Wilson coefficient C_9 in individual bins of q^2, using $B^0 \to K^{*0}\mu^+\mu^-$ measurements only. In particular, we consider separately the experimental data in bins below 2.5 GeV^2, between 2 and 4.3 GeV^2, between 4 and 6 GeV^2, and between 6 and 8.7 GeV^2 (the overlaps are due to the different binning unfortunately still used by different experiments). While the latter bin is not included in our NP fit as discussed in Sect. 2, we include it here as we are explicitly interested in the hadronic effects mimicking a shift in C_9. The results are shown in the left plot of Fig. 3. While the significance of the tension is more pronounced in the region above 4 GeV^2, this is not surprising as the observables are more sensitive to C_9 in this region. At 1σ, the fits are compatible with a flat q^2 dependence. Moreover, every single bin shows a preference for a shift in C_9, compatible with a constant new physics contribution of $C_9^{\mathrm{NP}} \sim -1$.

In the right plot of Fig. 3 we show results of fits that allow for helicity dependent shifts in the Wilson coefficient C_9, which we denote as ΔC_9^0 and ΔC_9^-. As before we split the data into q^2 bins. The fit results are perfectly consistent with a universal effect $\Delta C_9^0 = \Delta C_9^-$ for each individual q^2 bin. Furthermore, we also find that the fit results of the different q^2 bins are consistent with each other.

The absence of a q^2 and helicity dependence is intriguing, but cannot exclude a hadronic effect as the origin of the apparent discrepancies.

3.4 Predictions for LFU observables

As discussed, the "$B \to K^*\mu^+\mu^-$ anomaly" can be consistently described by new physics contributions to Wilson coefficients of the effective Hamiltonian (1). In order to determine the best-fit values for the various Wilson coefficients, we considered exclusively data on rare decays with muons in the final state. In this section, we use the obtained best-fit ranges from Sects. 3.1 and 3.2 to make predictions for theoretically clean lepton flavour universality (LFU) observables.

In contrast to hadronic effects, NP can lead to lepton flavour non-universality. NP predictions for LFU observables depend on additional assumptions how the NP affects $b \to see$ transitions. Well motivated are NP scenarios where $b \to see$ transitions remain approximately SM-like. This is realized for example in models that are based on the L_μ–L_τ gauge symmetry [61,62] and is also naturally the case in models based on partial compositeness [63]. We will therefore assume that $b \to see$ transitions are unaffected by NP. We use our fit results to map out the allowed ranges for a variety of LFU observables.

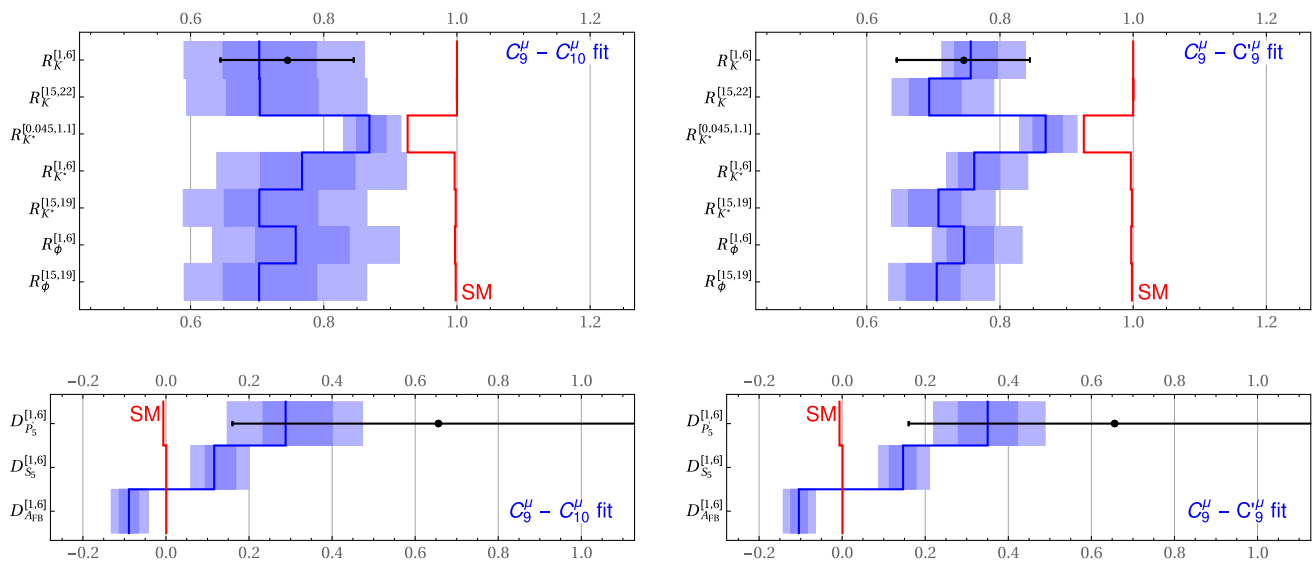We consider the following ratios of branching ratios [64, 65]:

Fig. 4 Predictions for lepton flavour universality ratios and differences in new physics models with muon specific contributions to C_9 and C_{10}, or C_9 and C_9'. The *superscripts* on the observables indicate the q^2 range in GeV^2. The red lines show the SM predictions. The 1σ and 2σ ranges in the NP scenarios are shown in *blue*. In *black* the LHCb measurement of R_K and the Belle measurement of $D_{P_5'}$

$$R_K = \frac{\text{Br}(B \to K\mu^+\mu^-)}{\text{Br}(B \to Ke^+e^-)} \quad R_{K^*} = \frac{\text{Br}(B \to K^*\mu^+\mu^-)}{\text{Br}(B \to K^*e^+e^-)},$$

$$R_\phi = \frac{\text{Br}(B_s \to \phi\mu^+\mu^-)}{\text{Br}(B_s \to \phi e^+e^-)}, \tag{4}$$

at low q^2 and at high q^2. The SM predictions for these ratios are unity to a very high accuracy up to kinematical effects at very low q^2 (cf. Appendix A.). We also consider differences of $B \to K^*\ell^+\ell^-$ angular observables as introduced in [62][1]

$$D_{P_5'} = P_5'(B \to K^*\mu\mu) - P_5'(B \to K^*ee), \tag{5}$$

$$D_{S_5} = S_5(B \to K^*\mu\mu) - S_5(B \to K^*ee), \tag{6}$$

$$D_{A_{\text{FB}}} = A_{\text{FB}}(B \to K^*\mu\mu) - A_{\text{FB}}(B \to K^*ee). \tag{7}$$

The angular observables P_5', S_5, and A_{FB} do not differ significantly from their SM predictions in the high q^2 region across the whole NP parameter space that provides a good fit of the $b \to s\mu\mu$ data. Therefore, we consider the above LFU differences only in the low q^2 region. In the SM the LFU differences vanish to an excellent approximation.

In Table 2 and in Fig. 4 we show the predictions for the LFU observables for two scenarios: (i) new physics in the Wilson coefficients C_9 and C_{10}; (ii) new physics in the Wilson coefficients C_9 and C_9'. We observe that in both scenarios, the observables R_K, R_{K^*} and R_ϕ are all suppressed with respect to their SM predictions. Since the best-fit regions of both scenarios correspond to similar values of the Wilson coefficients—a sizeable shift in C_9^μ and small effects in C_{10}^μ

or $C_9'^\mu$, respectively—the predictions for the observables are very similar both for the branching ratios and for the angular observables. The LHCb measurement of R_K [17] is in excellent agreement with our predictions. The recent results on $D_{P_5'}$ by Belle [36] are compatible with our predictions but still afflicted by large statistical uncertainties. If future measurements of any of the discussed LFU observables shows significant discrepancy with respect to SM predictions, it would be clear evidence for new physics.

4 Conclusions

In this paper, we have analyzed the status of the "$B \to K^*\mu^+\mu^-$ anomaly", i.e. the tension with SM predictions in various $b \to s\mu^+\mu^-$ processes, after the new measurements of $B \to K^*\mu^+\mu^-$ angular observables by ATLAS and CMS and including updated measurements by LHCb. We find that the significance of the tension remains strong. Assuming the tension to be due to NP, a good fit is obtained with a negative NP contribution to the Wilson coefficient C_9. Models predicting the NP contributions to the coefficients C_9 and C_{10} to be equal with an opposite sign give a comparably good fit.

We also studied the q^2 and helicity dependence of the nonstandard contribution to C_9. We find that the data agrees well with a q^2 and helicity independent new physics effect in C_9. A hadronic effect with these properties might appear surprising, but cannot be excluded as an explanation of the tensions.

Finally, again under the hypothesis of NP explaining the tensions, we provided a set of predictions for LFU observ-

---

[1] The observable $D_{P_5'}$ has recently also been considered in [66] and [36], where it is referred to as Q_5. See [67] for an alternative set of observables.
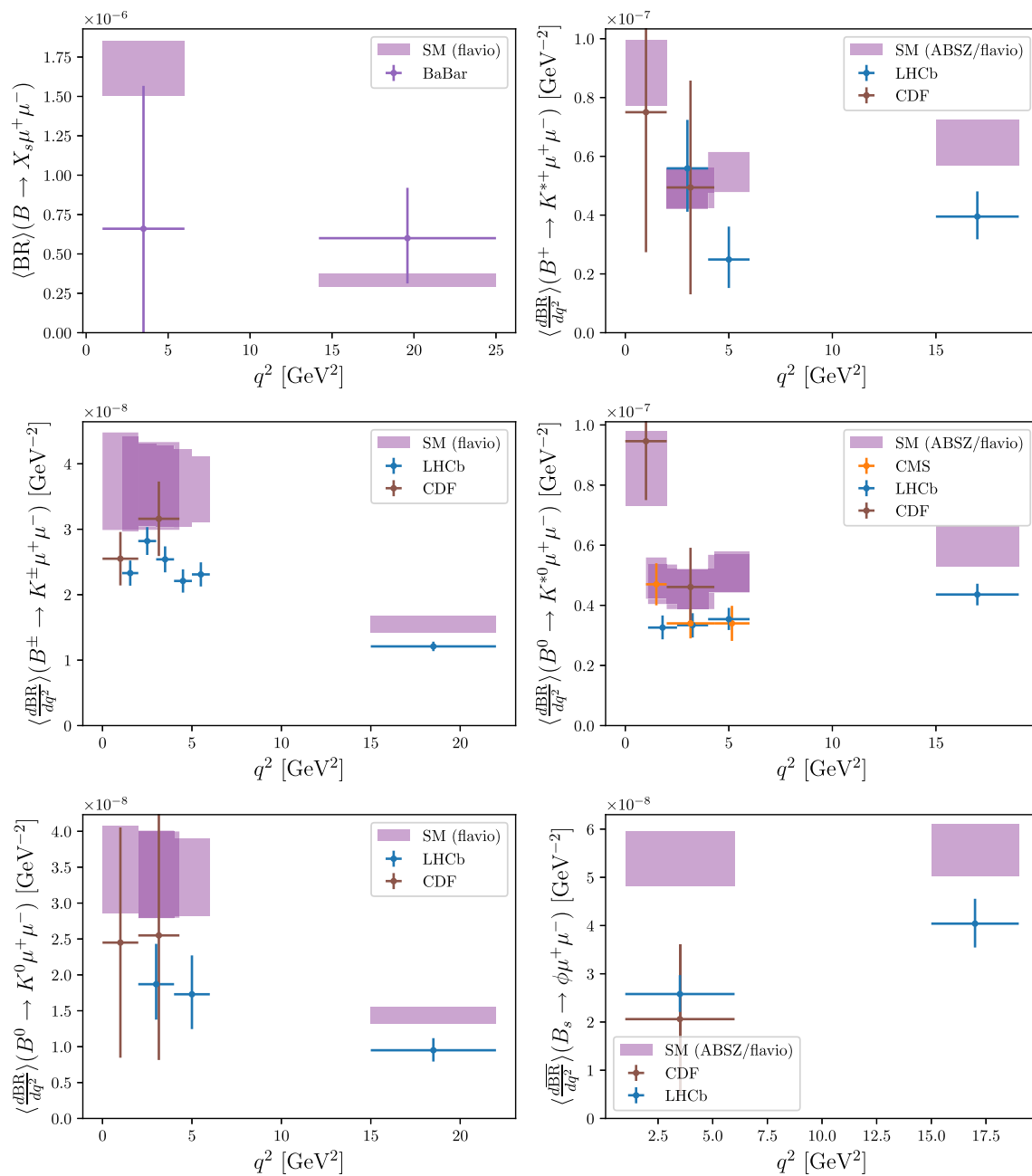
Fig. 5 Experimental measurements vs. SM predictions for the branching ratios. "ABSZ" refers to [20,32]

ables. Assuming that the new physics affects only $b \to s\mu\mu$ but not $b \to see$ transitions, we confirm that the latest $B \to K^*\mu^+\mu^-$ data shows astonishing compatibility with the LHCb measurement of the LFU ratio R_K. Future measurements of LFU observables that show significant deviations from SM predictions could not be explained by underestimated hadronic contributions but would be clear evidence for a new physics effect.
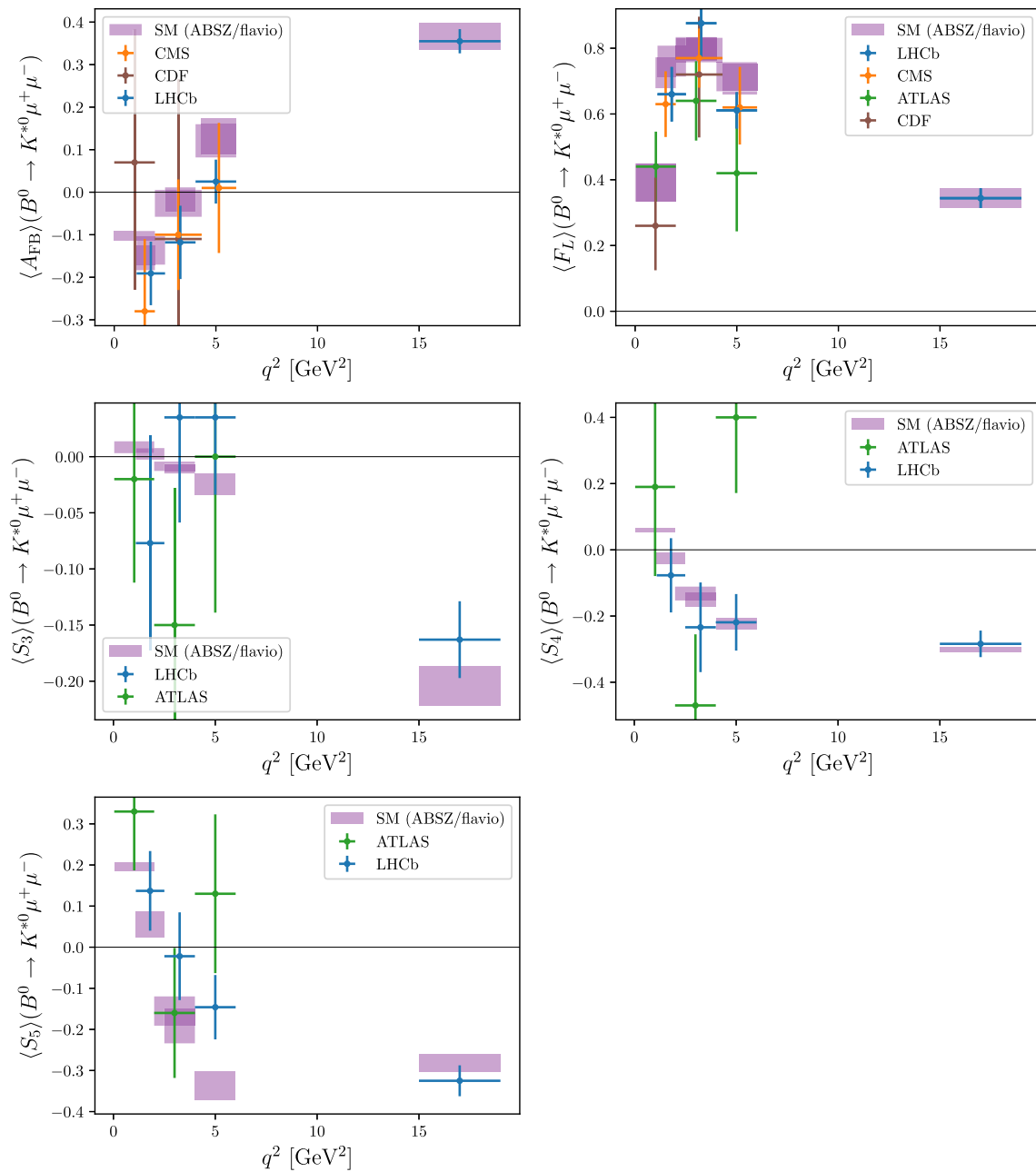
Fig. 6 Experimental measurements vs. SM predictions for the $B \to K^* \mu^+ \mu^-$ angular observables. "ABSZ" refers to [20,32]

A. Predictions

Figures 5, 6, 7 and 8 compare the binned experimental measurements to the SM predictions in the same bins, obtained with `flavio` version 0.21.2. We only show the bins included in our fits (cf. the discussion in Sect. 2). "ABSZ" refers to the predictions for $B \to V \ell^+ \ell^-$ observables in `flavio`, which

are based on the results of [20] (BSZ) for low q^2 and [32] (AS) for high q^2.

Table 3 shows the SM predictions for observables sensitive to violation of LFU. The uncertainties are parametric uncertainties only, i.e. it is assumed that final state radiation effects are simulated fully on the experimental side and QED corrections due to light hadrons are neglected (cf. [68]).
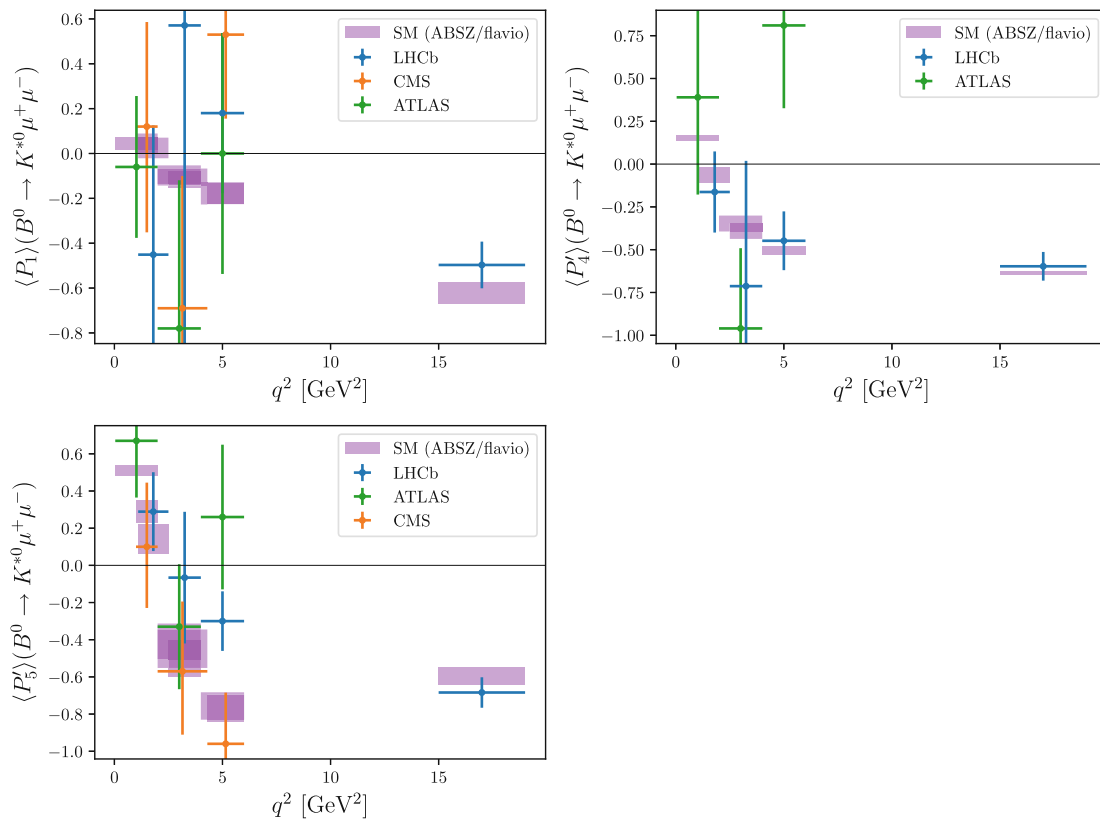
Fig. 7 Experimental measurements vs. SM predictions for the $B \to K^* \mu^+ \mu^-$ "optimized" observables. "ABSZ" refers to [20,32]
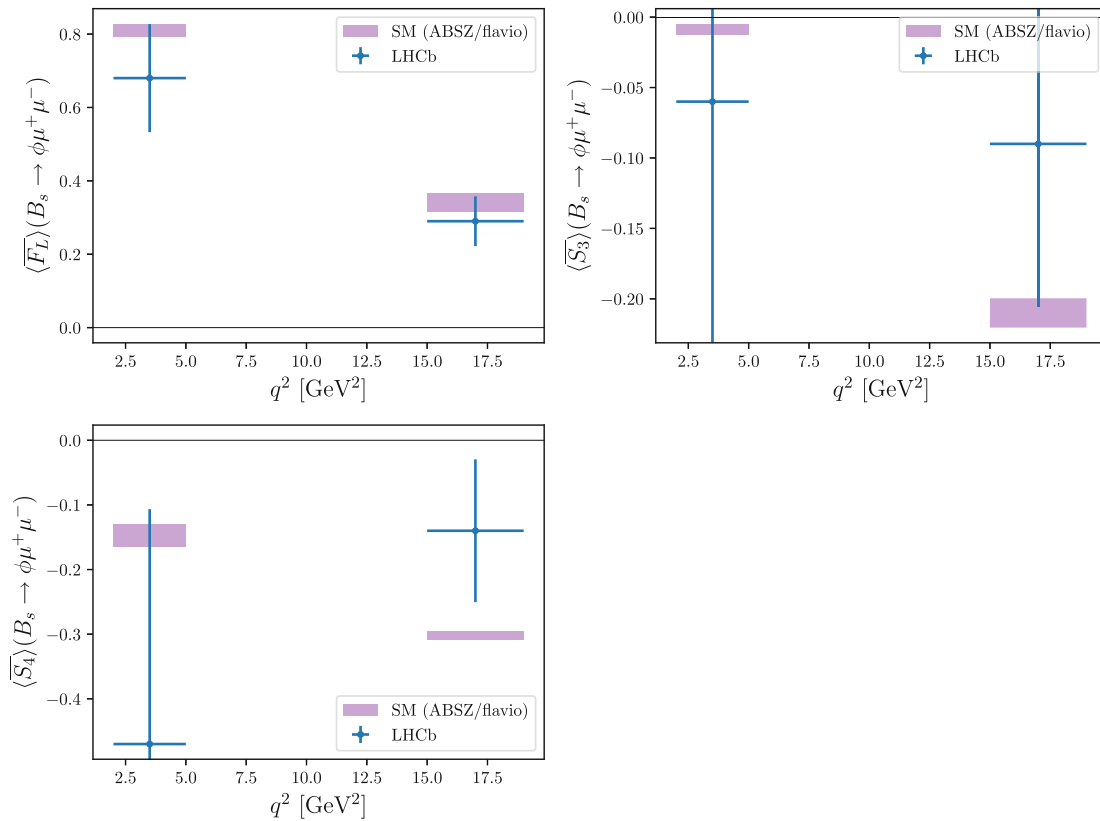

Fig. 8 Experimental measurements vs. SM predictions for the $B_s \to \phi \mu^+ \mu^-$ angular observables. "ABSZ" refers to [20,32]

Table 3 SM predictions for LFU observables in different q^2 bins. The D observables have been defined in Eq. (7)

	$q^2 \in [0.045, 1.1]$	$q^2 \in [1.1, 6.0]$	$q^2 \in [15.0, 19.0]$
$\mathcal{R}_{K^*}$	0.9259 (41)	0.9965 (6)	0.9981 (1)
$\mathcal{R}_\phi$	0.9299 (28)	0.9970 (2)	0.9981 (1)
$D_{P_5'}$	0.0936 (37)	-0.0064 (5)	-0.0008 (1)
D_{S_5}	-0.0402 (26)	0.0008 (4)	0.00022 (4)
$D_{A_{\mathrm{FB}}}$	0.0088 (5)	0.0008 (3)	-0.00028 (5)

References

1. F. Kruger, L.M. Sehgal, N. Sinha, R. Sinha, Angular distribution and CP asymmetries in the decays $\bar{B} \to K^- \pi^+ e^- e^+$ and $\bar{B} \to \pi^- \pi^+ e^- e^+$. Phys. Rev. D **61**, 114028 (2000). arXiv:hep-ph/9907386. [Erratum: Phys. Rev. D63,019901(2001)]
2. F. Kruger, J. Matias, Probing new physics via the transverse amplitudes of $B^0 \to K^{*0}(\to K^- \pi^+)l^+ l^-$ at large recoil. Phys. Rev. D **71**, 094009 (2005). arXiv:hep-ph/0502060
3. C. Bobeth, G. Hiller, G. Piranishvili, CP asymmetries in bar $B \to \bar{K}^*(\to \bar{K}\pi)\ell\ell$ and Untagged $\bar{B}_s$, $B_s \to \phi(\to K^+ K^-)\ell\ell$ decays at NLO. JHEP **07**, 106 (2008). arXiv:0805.2525
4. U. Egede, T. Hurth, J. Matias, M. Ramon, W. Reece, New observables in the decay mode $\bar{B}_d \to \bar{K}^{*0} l^+ l^-$. JHEP **11**, 032 (2008). arXiv:0807.2589
5. W. Altmannshofer, P. Ball, A. Bharucha, A.J. Buras, D.M. Straub, M. Wick, Symmetries and asymmetries of $B \to K^* \mu^+ \mu^-$ decays in the standard model and beyond. JHEP **01**, 019 (2009). arXiv:0811.1214
6. A. Bharucha, W. Reece, Constraining new physics with $B \to K^* \mu^+ \mu^-$ in the early LHC era. Eur. Phys. J. C **69**, 623–640 (2010). arXiv:1002.4310
7. S. Descotes-Genon, J. Matias, M. Ramon, J. Virto, Implications from clean observables for the binned analysis of $B \to K^* \mu^+ \mu^-$ at large recoil. JHEP **01**, 048 (2013). arXiv:1207.2753
8. Belle Collaboration, J.T. Wei et al., Measurement of the differential branching fraction and forward–backword asymmetry for $B \to K^{(*)} \ell^+ \ell^-$. Phys. Rev. Lett. **103**, 171801 (2009). arXiv:0904.0770
9. CDF Collaboration, T. Aaltonen et al., Measurements of the angular distributions in the decays $B \to K^{(*)} \mu^+ \mu^-$ at CDF. Phys. Rev. Lett. **108**, 081807 (2012). arXiv:1108.0695
10. BaBar Collaboration, J.P. Lees et al., Measurement of angular asymmetries in the decays $B \to K^* \ell^+ \ell^-$. Phys. Rev. D **93**(5), 052015 (2016). arXiv:1508.07960
11. S. Descotes-Genon, J. Matias, J. Virto, Understanding the $B \to K^* \mu^+ \mu^-$ anomaly. Phys. Rev. D **88**, 074002 (2013). arXiv:1307.5683
12. W. Altmannshofer, D.M. Straub, New physics in $B \to K^* \mu\mu$? Eur. Phys. J. C **73**, 2646 (2013). arXiv:1308.1501
13. F. Beaujean, C. Bobeth, D. van Dyk, Comprehensive Bayesian analysis of rare (semi)leptonic and radiative B decays. Eur. Phys. J. C **74**, 2897 (2014). arXiv:1310.2478. [Erratum: Eur. Phys. J. C74,3179(2014)]
14. T. Hurth, F. Mahmoudi, On the LHCb anomaly in B $\to K^* \ell^+ \ell^-$. JHEP **04**, 097 (2014). arXiv:1312.5267
15. LHCb Collaboration, R. Aaij et al., Differential branching fractions and isospin asymmetries of $B \to K^{(*)} \mu^+ \mu^-$ decays. JHEP **06**, 133 (2014). arXiv:1403.8044
16. LHCb Collaboration, R. Aaij et al., Angular analysis and differential branching fraction of the decay $B_s^0 \to \phi \mu^+ \mu^-$. JHEP **09**, 179 (2015). arXiv:1506.08777
17. LHCb Collaboration, R. Aaij et al., Test of lepton universality using $B^+ \to K^+ \ell^+ \ell^-$ decays. Phys. Rev. Lett. **113**, 151601 (2014). arXiv:1406.6482
18. R.R. Horgan, Z. Liu, S. Meinel, M. Wingate, Lattice QCD calculation of form factors describing the rare decays, $B \to K^* \ell^+ \ell^-$ and $B_s \to \phi \ell^+ \ell^-$. Phys. Rev. D **89**(9), 094501 (2014). arXiv:1310.3722
19. R.R. Horgan, Z. Liu, S. Meinel, M. Wingate, Rare B decays using lattice QCD form factors. PoS **LATTICE2014**, 372 (2015). arXiv:1501.00367
20. A. Bharucha, D.M. Straub, R. Zwicky, $B \to V \ell^+ \ell^-$ in the Standard Model from light-cone sum rules. JHEP **08**, 098 (2016). arXiv:1503.05534
21. S. Jäger, J. Martin Camalich, Reassessing the discovery potential of the $B \to K^* \ell^+ \ell^-$ decays in the large-recoil region: SM challenges and BSM opportunities. Phys. Rev. D **93**(1), 014028 (2016). arXiv:1412.3183
22. S. Descotes-Genon, L. Hofer, J. Matias, J. Virto, On the impact of power corrections in the prediction of $B \to K^* \mu^+ \mu^-$ observables. JHEP **12**, 125 (2014). arXiv:1407.8526
23. B. Capdevila, S. Descotes-Genon, L. Hofer, J. Matias, Hadronic uncertainties in $B \to K^* \mu^+ \mu^-$: a state-of-the-art analysis. arXiv:1701.08672
24. J. Lyon, R. Zwicky, Resonances gone topsy turvy - the charm of QCD or new physics in $b \to s \ell^+ \ell^-$? arXiv:1406.0566
25. M. Ciuchini, M. Fedele, E. Franco, S. Mishima, A. Paul, L. Silvestrini, M. Valli, $B \to K^* \ell^+ \ell^-$ decays at large recoil in the standard model: a theoretical reappraisal. JHEP **06**, 116 (2016). arXiv:1512.07157
26. V.G. Chobanova, T. Hurth, F. Mahmoudi, D. Martinez Santos, S. Neshatpour, Large hadronic power corrections or new physics in the rare decay $B \to K^* \ell\ell$? arXiv:1702.02234
27. A. Khodjamirian, T. Mannel, A.A. Pivovarov, Y.M. Wang, Charm-loop effect in $B \to K^{(*)} \ell^+ \ell^-$ and $B \to K^* \gamma$. JHEP **09**, 089 (2010). arXiv:1006.4945
28. M. Beylich, G. Buchalla, T. Feldmann, Theory of $B \to K^{(*)} \ell^+ \ell^-$ decays at high q^2: OPE and quark-hadron duality. Eur. Phys. J. C **71**, 1635 (2011). arXiv:1101.5118
29. A. Khodjamirian, T. Mannel, Y.M. Wang, $B \to K \ell^+ \ell^-$ decay at large hadronic recoil. JHEP **02**, 010 (2013). arXiv:1211.0234
30. S. Jäger, J. Martin Camalich, On $B \to V \ell\ell$ at small dilepton invariant mass, power corrections, and new physics. JHEP **05**, 043 (2013). arXiv:1212.2263
31. LHCb Collaboration, R. Aaij et al., Angular analysis of the $B^0 \to K^{*0} \mu^+ \mu^-$ decay using 3 fb^{-1} of integrated luminosity. JHEP **02**, 104 (2016). arXiv:1512.04442
32. W. Altmannshofer, D.M. Straub, New physics in $b \to s$ transitions after LHC run 1. Eur. Phys. J. C **75**(8), 382 (2015). arXiv:1411.3161
33. S. Descotes-Genon, L. Hofer, J. Matias, J. Virto, Global analysis of $b \to s \ell\ell$ anomalies. JHEP **06**, 092 (2016). arXiv:1510.04239
34. T. Hurth, F. Mahmoudi, S. Neshatpour, On the anomalies in the latest LHCb data. Nucl. Phys. B **909**, 737–777 (2016). arXiv:1603.00865
35. Belle Collaboration, A. Abdesselam et al., Angular analysis of $B^0 \to K^*(892)^0 \ell^+ \ell^-$, in Proceedings, LHCSki 2016 - A First Discussion of 13 TeV Results: Obergurgl, Austria, April 10–15, 2016, 2016. arXiv:1604.04042
36. Belle Collaboration, S. Wehle et al., Lepton-flavor-dependent angular analysis of $B \to K^* \ell^+ \ell^-$. Phys. Rev. Lett. **118**(11), 111801 (2017). arXiv:1612.05014
37. ATLAS Collaboration, Angular analysis of $B_d^0 \to K^* \mu^+ \mu^-$ decays in pp collisions at $\sqrt{s} = 8$ TeV with the ATLAS detector, Tech. Rep. ATLAS-CONF-2017-023, CERN, Geneva (2017)
38. CMS Collaboration, Measurement of the P_1 and P_5' angular parameters of the decay B$^0 \to K^{*0} \mu^+ \mu^-$ in proton–proton collisions at

$\sqrt{s}$ = 8 TeV. Tech. Rep. CMS-PAS-BPH-15-008, CERN, Geneva (2017)

39. W. Altmannshofer, P. Paradisi, D.M. Straub, Model-independent constraints on new physics in $b \rightarrow s$ transitions. JHEP **04**, 008 (2012). arXiv:1111.1257

40. W. Altmannshofer, D.M. Straub, Cornering new physics in $b \rightarrow s$ transitions. JHEP **08**, 121 (2012). arXiv:1206.0273

41. D. Straub et al., flav-io/flavio v0.21.2 Apr., 2017. https://flav-io.github.io/. doi:10.5281/zenodo.580247

42. W. Altmannshofer, C. Niehoff, D.M. Straub, $B_s \rightarrow \mu^+\mu^-$ as current and future probe of new physics. arXiv:1702.05498

43. A. Paul, D. M. Straub, Constraints on new physics from radiative B decays. arXiv:1608.02556

44. S. Jäger, K. Leslie, M. Kirk, A. Lenz, Charming new physics in rare B-decays and mixing? arXiv:1701.09183

45. CDF Collaboration, Updated branching ratio measurements of exclusive $b \rightarrow s\mu^+\mu^-$ decays and angular analysis in $B \rightarrow K^{(*)}\mu^+\mu^-$ decays. CDF public note 10894

46. CMS Collaboration, V. Khachatryan et al., Angular analysis of the decay $B^0 \rightarrow K^{*0}\mu^+\mu^-$ from pp collisions at $\sqrt{s}$ = 8 *TeV*. Phys. Lett. B **753**, 424–448 (2016). arXiv:1507.08126

47. C.M.S. Collaboration, V. Khachatryan et al., Angular analysis of the decay $B^0 \rightarrow K^{*0}\mu^+\mu^-$ from pp collisions at $\sqrt{s}$ = 8 TeV. HEPData (2016). doi:10.17182/hepdata.17057

48. LHCb Collaboration, R. Aaij et al., Measurements of the S-wave fraction in $B^0 \rightarrow K^+\pi^-\mu^+\mu^-$ decays and the $B^0 \rightarrow K^*(892)^0\mu^+\mu^-$ differential branching fraction. JHEP **11**, 047 (2016). arXiv:1606.04731

49. BaBar Collaboration, J.P. Lees et al., Measurement of the $B \rightarrow X_s l^+l^-$ branching fraction and search for direct CP violation from a sum of exclusive final states. Phys. Rev. Lett. **112**, 211802 (2014). arXiv:1312.5364

50. F. Beaujean, C. Bobeth, S. Jahn, Constraints on tensor and scalar couplings from $B \rightarrow K\bar{\mu}\mu$ and $B_s \rightarrow \bar{\mu}\mu$. Eur. Phys. J. C **75**(9), 456 (2015). arXiv:1508.01526

51. LHCb Collaboration, R. Aaij et al., Differential branching fraction and angular analysis of $\Lambda_b^0 \rightarrow \Lambda\mu^+\mu^-$ decays. JHEP **06**, 115 (2015). arXiv:1503.07138

52. S. Meinel, D. van Dyk, Using $\Lambda_b \rightarrow \Lambda\mu^+\mu^-$ data within a Bayesian analysis of $|\Delta B| = |\Delta S| = 1$ decays. Phys. Rev. D **94**(1), 013007 (2016). arXiv:1603.02974

53. LHCb Collaboration, R. Aaij et al., Measurement of the phase difference between short- and long-distance amplitudes in the $B^+ \rightarrow K^+\mu^+\mu^-$ decay. arXiv:1612.06764

54. M. Beneke, T. Feldmann, D. Seidel, Systematic approach to exclusive $B \rightarrow Vl^+l^-$, $V\gamma$ decays. Nucl. Phys. B **612**, 25–58 (2001). arXiv:hep-ph/0106067

55. J.A. Bailey et al., $B \rightarrow Kl^+l^-$ decay form factors from three-flavor lattice QCD. Phys. Rev. D **93**(2), 025026 (2016). arXiv:1509.06235

56. P. Ball, R. Zwicky, New results on $B \rightarrow \pi$, K, η decay formfactors from light-cone sum rules. Phys. Rev. D **71**, 014015 (2005). arXiv:hep-ph/0406232

57. M. Bartsch, M. Beylich, G. Buchalla, D.N. Gao, Precision flavour physics with $B \rightarrow K\nu\bar{\nu}$ and $B \rightarrow Kl^+l^-$. JHEP **11**, 011 (2009). arXiv:0909.1512

58. HPQCD Collaboration, C. Bouchard, G.P. Lepage, C. Monahan, H. Na, J. Shigemitsu, Rare decay $B \rightarrow K\ell^+\ell^-$ form factors from lattice QCD. Phys. Rev. D **88**(5), 054509 (2013). arXiv:1306.2384. [Erratum: Phys. Rev.D88,no.7,079901(2013)]

59. D. Du, A. X. El-Khadra, S. Gottlieb, A.S. Kronfeld, J. Laiho, E. Lunghi, R.S. Van de Water, R. Zhou, Phenomenology of semileptonic B-meson decays with form factors from lattice QCD. Phys. Rev. D **93**(3), 034005 (2016). arXiv:1510.02349

60. W. Altmannshofer, D.M. Straub, Implications of $b \rightarrow s$ measurements, in *Proceedings, 50th Rencontres de Moriond Electroweak Interactions and Unified Theories: La Thuile, Italy, March 14–21, 2015*, pp. 333–338, 2015. arXiv:1503.06199

61. W. Altmannshofer, S. Gori, M. Pospelov, I. Yavin, Quark flavor transitions in $L_\mu - L_\tau$ models. Phys. Rev. D **89**, 095033 (2014). arXiv:1403.1269

62. W. Altmannshofer, I. Yavin, Predictions for lepton flavor universality violation in rare B decays in models with gauged $L_\mu - L_\tau$. Phys. Rev. D **92**(7), 075022 (2015). arXiv:1508.07009

63. C. Niehoff, P. Stangl, D.M. Straub, Violation of lepton flavour universality in composite Higgs models. Phys. Lett. B **747**, 182–186 (2015). arXiv:1503.03865

64. G. Hiller, F. Kruger, More model independent analysis of $b \rightarrow s$ processes. Phys. Rev. D **69**, 074020 (2004). arXiv:hep-ph/0310219

65. G. Hiller, M. Schmaltz, Diagnosing lepton-nonuniversality in $b \rightarrow s\ell\ell$. JHEP **02**, 055 (2015). arXiv:1411.4773

66. B. Capdevila, S. Descotes-Genon, J. Matias, J. Virto, Assessing lepton-flavour non-universality from $B \rightarrow K^*\ell\ell$ angular analyses. JHEP **10**, 075 (2016). arXiv:1605.03156

67. N. Serra, R. Silva Coutinho, D. van Dyk, Measuring the breaking of lepton flavor universality in $B \rightarrow K^*\ell^+\ell^-$. Phys. Rev. D **95**(3), 035029 (2017). arXiv:1610.08761

68. M. Bordone, G. Isidori, A. Pattori, On the standard model predictions for R_K and R_{K^*}. Eur. Phys. J. C **76**(8), 440 (2016). arXiv:1605.07633